

Extraction of the spin-glass free-energy landscape from $1/f$ noise measurements

David C. Harrison ¹, E. Dan Dahlberg,¹ and Raymond L. Orbach ²

¹*School of Physics and Astronomy, The University of Minnesota, Minneapolis, Minnesota 55455, USA*

²*Texas Materials Institute, The University of Texas at Austin, Austin, Texas 78712, USA*

 (Received 15 June 2021; revised 27 December 2021; accepted 3 January 2022; published 11 January 2022)

The $1/f$ resistance noise has been measured in thin CuMn (13.5 at.%) spin-glass films. The temperature and frequency dependence have been analyzed in terms of the landscape of free-energy barriers. This analysis provides the full barrier distribution for various thin film thicknesses between 10 nm and 80 nm. The free-energy barrier height distribution's width and energy position have been determined. Contrary to previous models with fixed shape and energy, the free-energy landscape is described by a distribution of barriers that both shifts and changes shape as the temperature is reduced. The dependence of this distribution is in contrast with recent predictions. Using the fluctuation dissipation theorem, the $1/f$ measurements connect with χ'' , displaying agreement with other direct measurements of the latter.

DOI: [10.1103/PhysRevB.105.014413](https://doi.org/10.1103/PhysRevB.105.014413)

I. INTRODUCTION

After nearly 50 years of intense theoretical and experimental work, the fundamental dynamics of spin glasses are not fully understood. There has been notable progress recently, with numerical simulations for the first time exploring time and length scales comparable to experiment [1–11].

Recent experiments have shown that the 10–50 Oe applied fields typically used (e.g., Refs. [2–4,12,13]) to probe the spin-glass state measurably affect the energy landscape [3]. Previous work by Weissman and collaborators demonstrated that $1/f$ resistance noise measurements in metallic spin-glass systems are sensitive to the underlying magnetic dynamics [14–17] and, unlike more conventional measurements, can be made without an external magnetic field. We use $1/f$ noise measurements to directly probe the spin-glass energy landscape in mesoscale samples, without applying a field.

In our work, we present three results. First, we relate our measurements to the out-of-phase part of the ac susceptibility $\chi''(f, T)$ using the fluctuation-dissipation theorem (FDT) and compare to previous measurements of χ'' in thin spin-glass films. We observe the inferred χ'' curves at different frequencies cross at a temperature below the spin-glass freezing temperature, confirming an earlier result [12]. Second, we compare our measurements to recent measurements and analyses [1–10] and find that our measurements contrast with the recent work. Finally, we model the spin-glass energy landscape in a way that allows the shape of the energy barrier distribution to change with temperature, observing a striking dependence on film thickness.

The magnitude of the $1/f$ resistance noise of metallic spin glasses in the spin-glass state is more than an order of magnitude larger than the background noise [14]. For $T/T_f \gg 1$, where T_f is the freezing temperature, as defined later, local interference (LI) noise dominates: inelastic scattering events cause the conduction electrons to lose phase coherence, and

noise is generated by pairwise interference between scattering sites [14]. On the other hand, for $T \ll T_f$, the inelastic scattering length can be much larger than the elastic scattering length, and the noise is dominated by universal conductance fluctuations (UCFs), arising from interference between multiple Feynman paths [14]. Feng *et al.* (FBLM) worked out the UCF theory for spin glasses, finding a noise magnitude is proportional to $(\ell_{in}/\ell_{el})^{1.5}$ where ℓ_{in} and ℓ_{el} are the inelastic and elastic scattering lengths, respectively [18]. The growth of the inelastic scattering length as the temperature is reduced results in an approximately T^2 coupling factor between the resistance and magnetization noise, i.e., $S_M \sim T^2 S_R$ where S_M and S_R are the spectral densities of magnetic and resistance fluctuations, respectively [14,18]. This temperature dependence will be modified if the inelastic scattering length reaches the sample thickness, as it most likely does in our thinnest samples. We will be careful to point out where this could be a source of error, and why we do not believe that it is. Finally, we note that, by symmetry, the resistance is sensitive to a different set of spin-configuration fluctuations than the magnetization; the resistance is sensitive only to fluctuations of at least fourth order. This can be seen by noting that a global spin flip would not affect the resistance but would have a large effect on the magnetization. This is believed to explain why the resistance noise is only weakly sensitive to the application of a magnetic field [14].

Typical spectra at temperatures above, below, and near T_f are plotted for a 10 nm thick sample in Fig. 1. One clearly observes an increase in the magnitude of the resistance noise near T_f . The resistance noise continues to increase in magnitude as the temperature is reduced, even as the magnetic noise is expected to decrease (i.e., S_R is larger at $T/T_f = 0.56$ than at $T/T_f = 0.82$, which we would not expect for the magnetic noise). This is the result of the temperature-dependent coupling between the resistance and magnetic fluctuations.

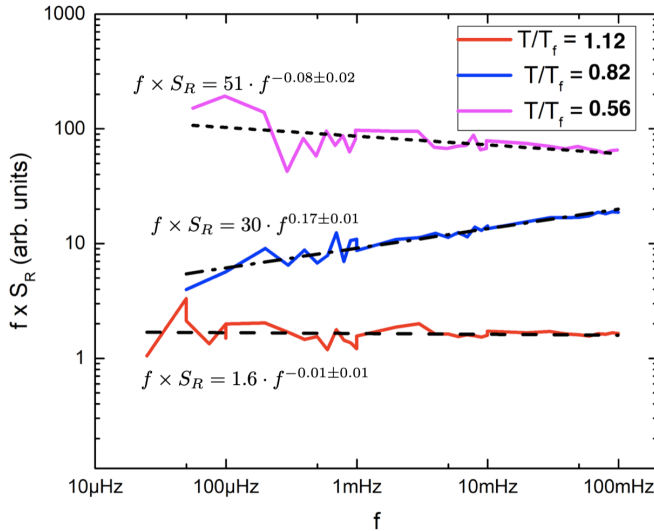


FIG. 1. Measured resistance spectral density, multiplied by frequency, in a 10 nm thick CuMn sample at three reduced temperatures. The noise magnitude increases by a factor of ~ 30 as the temperature is reduced, and the magnitude of the spectral exponent declines to ~ 0.83 near of T_f .

Figure 1 also shows a temperature-dependent spectral exponent, related to the shape of the barrier distribution. Noise with a spectral density $S_R \propto 1/f^\alpha$ where $0.7 \leq \alpha \leq 1.3$ can arise from a distribution of two-level systems [19]. The spectral exponent α is related to the shape of the distribution and the magnitude of the noise is related to the number density of barriers. In other words $|\alpha| = 1$, $|\alpha| < 1$, $|\alpha| > 1$ indicate a flat, negatively sloped, or positively sloped distribution. Assuming that the barrier distribution is temperature independent and that the noise is generated by thermally activated hopping over these barriers, one can relate the temperature dependence of the $1/f$ noise magnitude to the spectral exponent at each temperature with no free parameters. This is the Dutta-Horn picture [20]. In our spin-glass case, the Dutta-Horn picture as described does not fit our data, because the barriers have a strong temperature dependence; however, we can still use the basic reasoning with a single free parameter (which, following Ref. [16], we will call c) to account of the temperature dependence of the barriers.

II. SAMPLE PREPARATION AND EXPERIMENTAL TECHNIQUES

We dc sputtered mesoscale samples of thickness 10 nm, 18 nm, 25 nm, 40 nm, and 80 nm. We deposited in 2 mTorr Ar from several 3 in Cu_{86.5}Mn_{13.5} sputtering targets, stated to be 99.95% pure [21], at a typical deposition rate of approximately 0.5 nm/s. We capped our samples with a ~ 5 nm thick layer of rf-sputtered Al₂O₃ to prevent oxidation. Our substrates were Si₃N₄ with preexisting Au contacts, to allow for low resistance, low noise electrical contact. Following the deposition, we used electron-beam lithography and a standard hard-mask technique to create the noise samples as Wheatstone bridges, described elsewhere [11]. Additionally,

we simultaneously deposited large-area witness films for conventional measurements of T_f .

The ac technique that we used for our noise measurements was developed by Scofield [22] and first applied to metallic spin-glass systems by Weissman and his group [14–17]. Briefly, all electronics—including the amplifiers needed to measure small resistance changes—produce $1/f$ noise at low frequencies. Typically, this $1/f$ noise is larger in magnitude than the $1/f$ noise produced by our spin-glass systems. However, by passing an ac current (at, e.g., ~ 40 Hz) through our spin-glass devices and demodulating the resulting voltage signal with a lock-in amplifier, the lock-in contributes (white) noise near the demodulation frequency, well away from where the low-frequency $1/f$ amplifier noise becomes dominant. The lock-in output is sent to a computer to compute the voltage spectral density, which can be converted to a resistance spectral density using Ohm’s law. By patterning our devices as Wheatstone bridges with arms close to one another, we mitigate against both temperature fluctuations (a temperature fluctuation will affect each arm comparably, and largely cancel out) and current fluctuations.

For our noise measurements, we warmed above the bulk spin-glass transition temperature, T_g , and then rapidly cooled to a measurement temperature below the freezing temperature (dependent upon the film thickness). This procedure was repeated for each temperature of our $1/f$ noise measurements. Some of the measurements were made in a system with a greater than 10 K/min cooling rate, while others were made in a closed-cycle system with a slower 2 K/min cooling rate. One sample was measured both ways; the results were consistent between the two protocols and refrigerators, within experimental error.

For conventional measurements of the spin-glass freezing temperature, we measured the zero-field cooled (ZFC) magnetization of our witness films in a 10 Oe applied field, using commercially built Quantum Design MPMS systems. We approximate the freezing temperature of these films as the temperature corresponding to the peak of the ZFC magnetization. Despite the large area (>100 cm²) of these films, given the small thicknesses, the resulting volume was too low to determine T_f to better than ~ 1 K or to accurately measure the frequency dependence of T_f . This clearly demonstrates the advantages of using the noise technique, which enables us to measure this dependence accurately for samples with volumes much smaller than could be measured in more conventional ways.

III. CURVE CROSSING CONFIRMATION

The FDT, i.e., $S_M(f) = (k_B T / f) \chi''(f, T)$, has been demonstrated to be relevant to spin glasses [23] in spite of their nonergodic dynamics. We use our measured S_R to compute S_M and then use the FDT to compute the imaginary part of the magnetic susceptibility, $\chi''(f, T)$. In Fig. 2, we show the inferred $\chi''(f, T)$ for a 10 nm thick sample, and observe that the curves at different frequencies cross at a temperature below T_f . This implies that the peak of the barrier distribution is producing relaxation times within our measurement bandwidth, and never occurs in bulk films, but previously was observed in a 2 nm thick CuMn (13.5 at.%) sample [12].

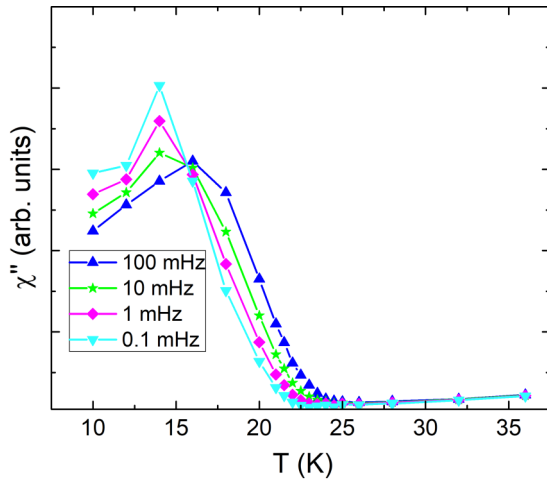


FIG. 2. χ'' for a 10 nm thick sample, derived using the FDT. Magnetometry indicates $T_f \approx 26$ K.

The qualitative agreement between these measurements and earlier measurements of $\chi''(f, T)$ lends credibility to the more quantitative comparisons we make in Sec. IV.

We note that the crossing of the inferred curves does not depend on the temperature dependence of the coupling. The crossing temperature is the result of the frequency dependence of the noise, occurring when the magnitude of the measured spectral exponent goes from less than to greater than unity. Physically, this corresponds to the peak in relaxation rates passing through our experimental window.

IV. COMPARISON WITH RECENT WORK

The recent progress [2,3] on spin-glass dynamics has been made through simulations and experimental results consistent with a correlation length growing according to

$$\xi(t, T) = c_1 a_0 (t/\tau_0)^{c_2 T/T_g}, \quad (1)$$

where a_0 is the average spacing between magnetic dopants; τ_0 is taken to be $\sim \hbar/k_B T_g$; T_g is the bulk spin-glass transition temperature; c_1 is a constant found to be approximately 1.5; and $c_2 = 1/Z_c$ (Z_c is the dynamical exponent) and depends on whether the dynamics are governed by the fixed point at T_g ($c_2 = 1/6.67$) or the fixed point at $T = 0$ (c_2 is temperature dependent and found to be approximately 0.104 over our typical range of temperature measurement [7]). The maximum barrier associated with the spin-glass state grows with time according to,

$$\frac{\Delta_{\max}(t, T)}{k_B T_g} = \frac{1}{c_2} \left[\ln \left(\frac{\xi(t, T)}{a_0} \right) - \ln c_1 \right]. \quad (2)$$

In thin film studies at sufficiently high temperatures, $\xi(t, T)$ can grow to the film thickness on experimental timescales. Thereafter, it can grow no further perpendicular to the plane. An analysis neglecting in-plane growth then results in a maximum barrier height that is temperature independent and set by the film thickness, \mathcal{W} , alone,

$$\frac{\Delta_{\max}(\mathcal{W})}{k_B T_g} = \frac{1}{c_2} \left[\ln \left(\frac{\mathcal{W}}{a_0} \right) - \ln c_1 \right]. \quad (3)$$

The apparent freezing temperature is then set by the experimental timescale, t_{exp} according to,

$$t_{\text{exp}} \sim \tau_0 \exp(\Delta_{\max}/T_f). \quad (4)$$

The data from Refs. [2,3] are well fitted by this form. However, measurements of the magnetic field dependence of the maximum barrier height in Ref. [3] strongly suggest that the correlated regions are not spherical, but pancakelike, with an in-plane correlation length approximately one order of magnitude larger than the perpendicular correlation length for a 20 nm thick film. It is an open question how the in-plane correlation length growth affects the barrier heights. It is important to note that, in order to use this analysis [Eqs. (1)–(4)], a specific cooling protocol must be used. The temperature must be cycled above the bulk T_g between each measurement and then rapidly quenched to the measurement temperature.

This greatly differs from earlier analyses (e.g., Refs. [12,13], among many others), which assumed the phase transition occurs at a reduced temperature (as low as 0 K for a two-dimensional film) and the dynamical properties of the freezing (e.g., the frequency dependence of T_f) were set by the two-dimensional growth of the correlation length. In contrast, in the more recent analysis, it was assumed that near T_f , the critical point at the bulk T_g governs the growth of the spin-glass correlation length until it reaches the film thickness, after which it was assumed that any further growth did not affect the dynamics. Here, the freezing temperature is set by the film thickness alone. Excellent agreement with numerical simulations vindicated this approach [10].

We quantitatively compare with both the earlier work [12,13,16] and the more recent analyses [1–3] by considering the frequency dependence of T_f . We compute $b^{-1} \equiv d \ln T_f / d \ln f$ [16] for the previously published data. For our noise data, we calculate

$$c = - \frac{\partial \ln S_R}{\partial \ln T} \left(1 + \frac{\partial \ln S_R}{\partial \ln f} \right)^{-1}, \quad (5)$$

which is essentially equivalent to b when evaluated at T_f [16]. For temperature-independent barriers, both b and c are approximately 34. Our form for c assumes a T^2 coupling between the resistance fluctuations and the magnetic fluctuations; if the inelastic scattering length has reached the film thickness, as it likely has near and below T_f in our thinnest film, there will be a small ($\sim 5\%$) correction that does affect our comparison with previous measurements. Well away from T_f , this correction could be much larger, as is the uncertainty in c .

In the recent analyses [1–3], Δ_{\max} is fixed by the film thickness and is temperature-independent, so $b \approx 34$. From our measurements, $c \approx 75, 90, 100, 150, 170$ for the 10 nm, 18 nm, 25 nm, 40 nm, and 80 nm films, respectively. This is inconsistent with the recent work.

Our computed values are qualitatively consistent with Ref. [12,13]; the agreement is improved by assuming there are nonmagnetic layers (of combined thickness ~ 6 nm) at the surfaces of our films. This is supported by our measurements of T_f , approximated by the peak of the ZFC magnetization (in a 10 Oe applied field) in our witness films. The measured T_f values are smaller than the T_f values measured in

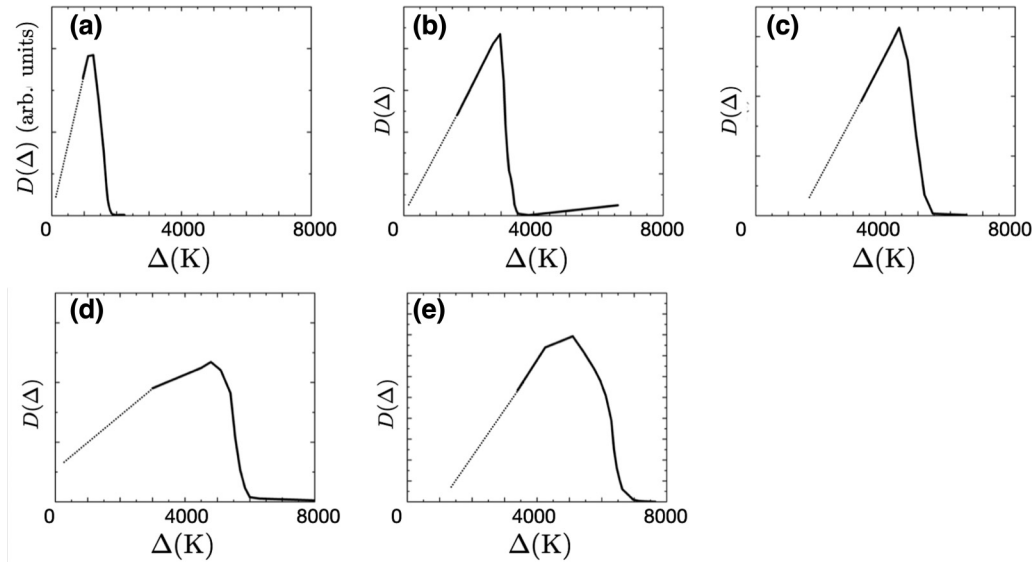


FIG. 3. Barrier distributions at $T = 0$ for our five thicknesses, based on our measurements of $S_R(f, T)$ for film thicknesses: (a) 10 nm, (b) 18 nm, (c) 25 nm, (d) 40 nm, and (e) 80 nm. The bold portions fall within our measurement bandwidth. The dashed portions are an extrapolation to guide the eye.

multilayer films with metallic spacer layers, previously observed in Ref. [24]. Notably, $c \approx 75$ in our thinnest film, consistent with Ref. [12] and the droplet model prediction for a two-dimensional film, and in our two thickest films, $c \approx 150$ and $c \approx 170$, similar to $b^{-1} \approx 190$ for the 50 nm thick film in Ref. [12]. For completeness, we find $T_f = 26$ K, 32 K, 40 K, 46 K, and 49 K for the 10 nm, 18 nm, 25 nm, 40 nm, and 80 nm films, respectively.

It is not clear why our data demonstrate reasonable agreement with Refs. [12,13], as the recent analysis would predict that our cooling protocol should give very different results (Ref. [1] was able to reconcile Refs. [12,13] by assuming a cooling protocol in which the temperature was not cycled above the bulk T_g between measurements). This discrepancy between our results and Eq. (3) warrants future consideration; the observation of barriers fixed by the film thickness is a prerequisite for many interesting experiments.

V. BARRIER DISTRIBUTION CALCULATIONS

Having demonstrated a temperature-dependent barrier distribution, we use our noise measurements to calculate the spin-glass energy landscape. In the simplest picture, the spin-glass state has been modeled as a collection of superparamagnetic clusters with a fixed, temperature-independent distribution of blocking temperatures. However, doing this requires an unphysical attempt frequency (10^{100} Hz or larger), indicating the inadequacy of this model and that the transition is cooperative, with barriers growing as the temperature is reduced [25,26]. This is consistent with our data. However, any comparison of our data with earlier data [12,13,25,26] is tenuous, as the cooling protocol used was not fully specified, and, as previously mentioned, the spin-glass energy barriers strongly depend on the cooling protocol [1]. When it is possible to fit the measurements with an unphysical attempt frequency, we can instead consider the distribution of blocking temperatures of fixed shape, shifting towards larger

blocking temperatures as the sample temperature is reduced. From this analysis, we can model the energy barrier distribution as a function of temperature. The parameters b and c quantify how rapidly this distribution shifts with temperature.

We use the Dutta-Horn analysis employed by Fenimore and Weissman [16] to compute the shape of this energy barrier distribution and calculate c [given in Eq. (5)]. Our data can be fitted by a distribution with a linear temperature dependence. With the shape of this distribution for each thickness, we extrapolate to $T = 0$ taking the temperature dependence of the barriers as $\Delta(T) = \Delta(0) + (c - 34)k_B T$. As can be seen, both the energy of the peak of the distribution and the width of the distribution increase with sample thickness. In Fig. 4,

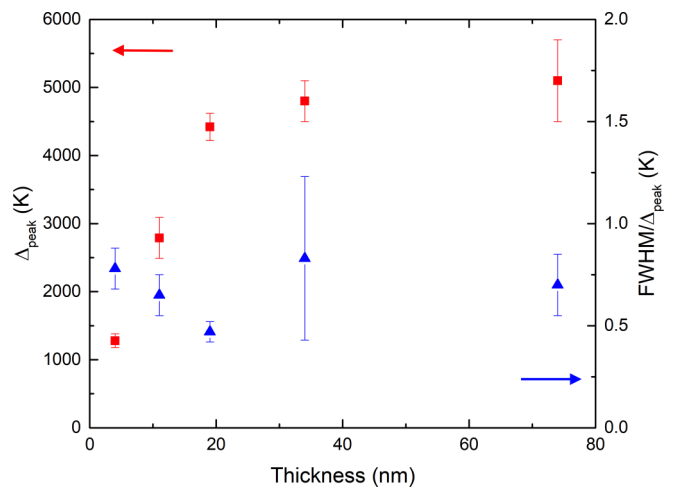


FIG. 4. Position of peak and $\text{FWHM}/\Delta_{\text{peak}}$ in Fig. 3 vs film thickness. The peak position increases with thickness. In our range of thicknesses, the data can be fit with a logarithmic dependence. Within experimental uncertainty, the $\text{FWHM}/\Delta_{\text{peak}}$ is independent of thickness.

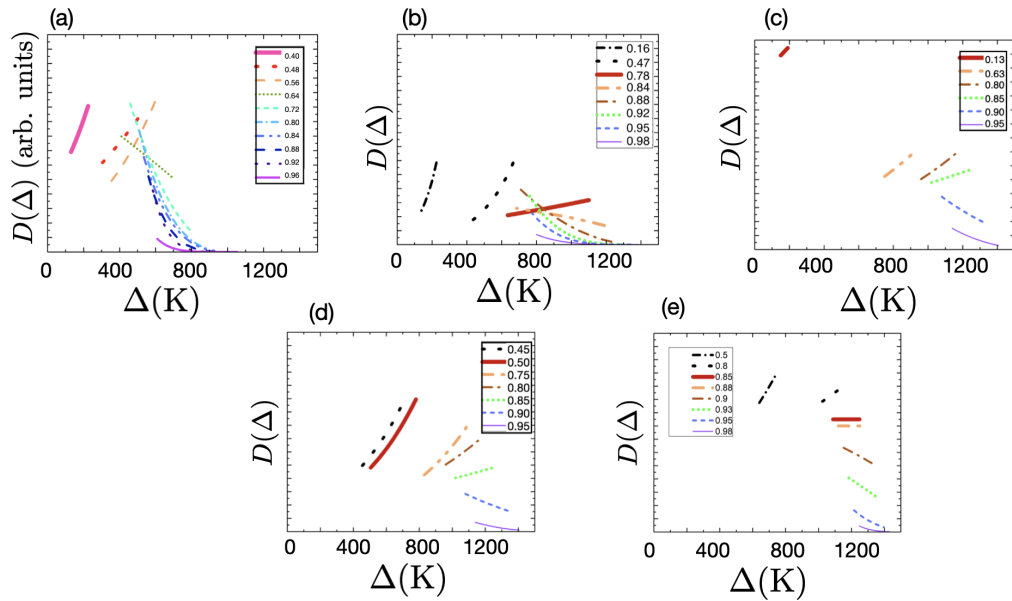


FIG. 5. Extracted barrier distributions for film thicknesses: (a) 10 nm, (b) 18 nm, (c) 25 nm, (d) 40 nm, and (e) 80 nm. Each segment corresponds to a different reduced temperature T/T_f and the finite segment length is the result of the finite experimental bandwidth, explained in the text. All distributions have an implied peak, with larger thicknesses having a peak at a larger barrier height. Additionally, the larger thicknesses exhibit a stronger temperature dependence than the thinner samples.

we plot the peak of that distribution and the full-width at half-maximum, normalized by the peak position.

The aforementioned (Dutta-Horn) model fixes the shape of the barrier distribution, and while it models our data well in the vicinity of T_f , at lower temperatures the agreement is poor, and our measured spectral exponent is always larger in magnitude than would be expected from this model. In principle, it might be possible to improve the agreement by allowing c to vary with temperature and by altering the temperature dependence of the coupling between the resistance and magnetization noise. However, the uncertainty in c grows very large near the temperature where the magnitude of the spectral exponent is unity, and the coupling between resistance and magnetization is not known to sufficient precision for this to be helpful. For these reasons, we wished to model our data in another way. As with measurements of χ'' [12,13,25,26], our noise measurements directly probe the distribution of relaxation times in our system. In contrast with the Dutta-Horn analysis, we make no explicit assumption about the shape of our barrier distribution. Instead, from our data, we extract a segment of the barrier distribution at each measurement temperature, making two assumptions. The first is that the dynamics are driven by thermally activated hopping over energy barriers, with a physically reasonable attempt time on the order of $\sim \hbar/k_B T_g$, and that spectrum is a superposition of these two-level systems. There is evidence the systems are not two level but many level and they interact [17]; however, this simplification gives a tractable model. The second assumption is that only barriers within one decade of frequency of our measurement bandwidth contribute substantially to the spectrum within our bandwidth. This is likely not well satisfied, as the high density of barriers near the peak of the distribution ostensibly always plays a role. However, this assumption allows our distribution to both shift and change shape as the

temperature is reduced, in contrast with earlier models that fix the shape. This second assumption explains why we extract only a portion of the barrier profile at each measurement temperature. If the largest (smallest) frequency within our measurement bandwidth is $f_{\max}(\min) = f_0 \exp[-\Delta/k_B T]$, then the smallest (largest) barrier falling within that bandwidth is given by $\Delta = k_B T \ln(f_0/f_{\max}(\min))$. Smaller (larger) barriers result in faster (slower) transitions, falling outside of our bandwidth. For our measurements, typically f_{\max} is between 100–500 mHz and f_{\min} is between 10–100 μ Hz.

Our results are displayed in Fig. 5 for five thicknesses. The segments were computed by adding Lorentzian spectra, with a distribution that is nonzero between one decade lower than f_{\min} and one decade larger than f_{\max} . We used a T^2 coupling between the magnetic and resistance fluctuations, as described earlier in the paper. We modified the distribution by hand, until it reproduced our experimental data to within experimental uncertainty. Additionally, we added in a nonmagnetic background spectrum with a linear temperature dependence. This describes the noise well above T_f and is much smaller than the magnetic noise at low temperatures. The background spectrum contributes substantially only near T_f ; at lower frequencies, the magnetic noise is much larger. The range of temperature near T_f where the background is a substantial contribution is narrow, and, e.g., a constant temperature dependence would not have a large effect on our distributions. The clear change in the sign of the slope of the observed segments of $D(\Delta)$ in Fig. 5 as the temperature is changed indicates a peak in the distribution appearing to pass through our measurement bandwidth at temperatures near where the sign changes. The change in temperature dependence as a function of thickness is also striking. The distribution for the 10 nm thick sample has a much weaker temperature dependence than the 80 nm thick sample. This is evidenced by the fact that at

many temperatures near T_f the probed portion of the barrier distribution has similar, overlapping density for the 10 nm thick sample, where there is no such overlap in the thicker samples. A direct comparison with the Dutta-Horn analysis cannot be made, as we have no means of extracting the portion of the barrier distribution outside of our measurement bandwidth. However, our model reproduces our measured data, within experimental error, at all temperatures.

VI. CONCLUSIONS

In conclusion, we have explicitly extracted a temperature-dependent energy barrier distribution, consistent with our measured $1/f$ noise data, in CuMn thin films. We have extracted the shape, width, and energy position of the distribution versus temperature for films of five thicknesses between 10–80 nm. Previous analyses [1,12,13] considered only the temperature and frequency dependences of the peak of the distribution, whereas we display the full shape and position. Our distributions exhibit a temperature-dependence consistent with earlier measurements [12,13], despite using a cooling protocol suitable for comparison with simulations that suggest temperature-independent barriers [1,2,4]. More work is needed to understand the apparent discrepancy between our measurements and those of Refs. [2,3]. Additionally, using

the FDT, we show that our noise measurements reproduce the most notable feature of the temperature and frequency dependence of χ'' in the thinnest CuMn films. This both confirms the previous result and lends credibility to our interpretation of our measurements as roughly equivalent to more conventional magnetometry, despite probing a different set of spin configurations.

ACKNOWLEDGMENTS

This work was supported by the U.S. Department of Energy, Office of Science, Basic Energy Sciences, under Award DE-SC0013599. Parts of this work were carried out in the Characterization Facility, University of Minnesota, which receives partial support from NSF through the MRSEC program. Portions of this work were conducted in the Minnesota Nano Center, which is supported by the National Science Foundation through the National Nanotechnology Coordinated Infrastructure (NNCI) under Award No. ECCS-2025124. Part of this work was performed at the Institute for Rock Magnetism (IRM) at the University of Minnesota. The IRM is a U.S. National Multi-user Facility supported through the Instrumentation and Facilities program of the National Science Foundation, Earth Sciences Division, under Award No. 1642268 (NSF EAR-1642268), and by funding from the University of Minnesota.

-
- [1] S. Guchhait, G. G. Kenning, R. L. Orbach, and G. F. Rodriguez, *Phys. Rev. B* **91**, 014434 (2015).
 - [2] Q. Zhai, D. C. Harrison, D. Tennant, E. D. Dahlberg, G. G. Kenning, and R. L. Orbach, *Phys. Rev. B* **95**, 054304 (2017).
 - [3] Q. Zhai, D. C. Harrison, and R. L. Orbach, *Phys. Rev. B* **96**, 054408 (2017).
 - [4] S. Guchhait and R. L. Orbach, *Phys. Rev. Lett.* **118**, 157203 (2017)
 - [5] Janus Collaboration, M. Baity-Jesi, E. Calore, A. Cruz, L. A. Fernandez, J. M. Gil-Navarion, A. Gordillo-Guerrero, D. Iniguez, A. Maiorano, E. Marinari, V. Martin-Mayor, J. Monforte-Garcia, A. Munoz-Sudupe, D. Navarro, G. Parisi, S. Perez-Gaviro, F. Ricci-Tersenghi, J. J. Ruiz-Lorenzo, S. F. Schifano, B. Seoane, A. Tarancon, R. Tripiccion, and D. Yllanes, *Phys. Rev. Lett.* **118**, 157202 (2017).
 - [6] G. G. Kenning, D. M. Tennant, C. M. Rost, F. G. da Silva, B. J. Walters, Q. Zhai, D. C. Harrison, E. D. Dahlberg, and R. L. Orbach, *Phys. Rev. B* **98**, 104436 (2018).
 - [7] Q. Zhai, V. Martin-Mayor, D. L. Schlagel, G. G. Kenning, and R. L. Orbach, *Phys. Rev. B* **100**, 094202 (2019).
 - [8] Q. Zhai, I. Paga, M. Baity-Jesi, E. Calore, A. Cruz, L. A. Fernandez, J. M. Gil-Narvion, I. Gonzalez-AdalidPemartin, A. Gordillo-Guerrero, D. Iniguez, A. Maiorano, E. Marinari, V. Martin-Mayor, J. Moreno-Gordo, A. Munoz-Sudupe, D. Navarro, R. L. Orbach, G. Parisi, S. Perez-Gaviro, F. Ricci-Tersenghi, J. J. Ruiz-Lorenzo, S. F. Schifano, D. L. Schlagel, B. Seoane, A. Tarancon, R. Tripiccion, and D. Yllanes, *Phys. Rev. Lett.* **125**, 237202 (2020).
 - [9] L. A. Fernandez, E. Marinari, V. Martin-Mayor, G. Parisi, and J. J. Ruiz-Lorenzo, *Phys. Rev. B* **94**, 024402 (2016)
 - [10] L. A. Fernandez, E. Marinari, V. Martin-Mayor, I. Paga, and J. J. Ruiz-Lorenzo, *Phys. Rev. B* **100**, 184412 (2019).
 - [11] D. C. Harrison, E. D. Dahlberg, and R. L. Orbach, *Phys. Rev. B* **100**, 064411 (2019).
 - [12] P. Granberg, P. Nordblad, P. Svedlindh, L. Lundgren, R. Stubi, G. G. Kenning, D. L. Leslie-Pelecky, J. Bass, and J. Cowen, *J. Appl. Phys.* **67**, 5252 (1990).
 - [13] L. Sandlund, P. Granberg, L. Lundgren, P. Nordblad, P. Svedlindh, J. A. Cowen, and G. G. Kenning, *Phys. Rev. B* **40**, 869(R) (1989).
 - [14] N. E. Israeloff, M. B. Weissman, G. J. Nieuwenhuys, and J. Kosiorowska, *Phys. Rev. Lett.* **63**, 794 (1989).
 - [15] N. E. Israeloff and G. B. Alers, and M. B. Weissman, *Phys. Rev. B* **44**, 12613 (1991).
 - [16] P. W. Fenimore and M. B. Weissman, *J. Appl. Phys.* **85**, 8317 (1999).
 - [17] K. A. Meyer and M. B. Weissman, *Phys. Rev. B* **51**, 8221 (1995).
 - [18] S. Feng, A. J. Bray, P. A. Lee, and M. A. Moore, *Phys. Rev. B* **36**, 5624 (1987).
 - [19] B. N. Costanzi and E. D. Dahlberg, *Phys. Rev. Lett.* **119**, 097201 (2017).
 - [20] P. Dutta and P. M. Horn, *Rev. Mod. Phys.* **53**, 497 (1981).
 - [21] Purchased from ACI Alloys.
 - [22] J. H. Scofield, *Rev. Sci. Instr.* **58**, 985 (1987).
 - [23] W. Reim, R. H. Koch, A. P. Malozemoff, M. B. Ketchen, and H. Maletta, *Phys. Rev. Lett.* **57**, 905 (1986).
 - [24] G. G. Kenning, J. Bass, W. P. Pratt, Jr., D. Leslie-Pelecky, L. Hoines, W. Leach, M. L. Wilson, R. Stubi, and J. A. Cowen, *Phys. Rev. B* **42**, 2393 (1990).
 - [25] C. A. M. Mulder, A. J. van Duynveldt, and J. A. Mydosh, *Phys. Rev. B* **23**, 1384 (1981).
 - [26] L. Lundgren, P. Svedlindh, and O. Beckman, *J. Magn. Magn. Mater.* **25**, 33 (1981).